Faraday Discussions

Accepted Manuscript

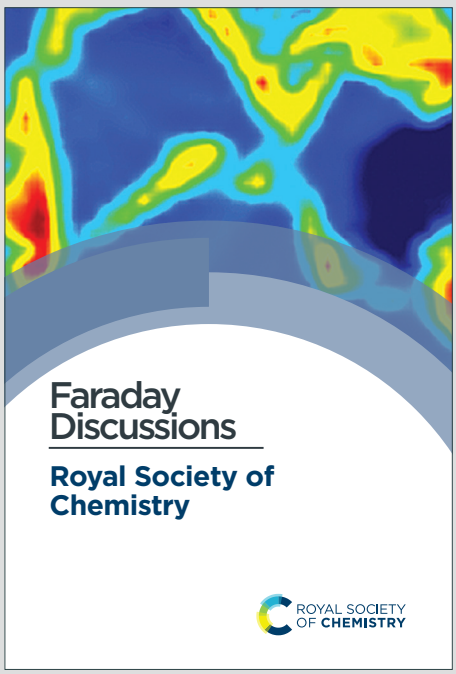

This article can be cited before page numbers have been issued, to do this please use: J. F. Schuster, Q. Hu, L. King, A. L. Lapidus, C. A. Hall, L. Nyholm and R. Younesi, *Faraday Discuss.*, 2026, DOI: 10.1039/D6FD00038J.

ROYAL SOCIETY OF CHEMISTRY

www.rsc.org/faraday_d

Faraday Discussions

View Article Online
DOI: 10.1039/D6FD00038J

PAPER

Understanding the stability of the solid electrolyte interphase formed by vinylene carbonate and fluoroethylene carbonate in sodium-ion batteries

Jan Felix Schuster*[1], Qihan Hu[1], Laura King[1], Alexandre Linas Lapidus[1], Charles Aram Hall[1], Leif Nyholm[1], Reza Younesi*[1]

Received 00th January 20xx, Accepted 00th January 20xx
DOI: 10.1039/x0xx00000x

The formation of a stable solid electrolyte interphase (SEI) in sodium-ion batteries is a challenge which is usually solved by introducing film-forming electrolyte additives. The functions and decomposition of common additives like vinylene carbonate (VC) and flouroethylene carbonate (FEC) are not fully understood and yield different results in full- and half-cells. This study reveals that the electrochemical reduction of an electrolyte solution based on 1 M $NaPF_6$ dissolved in ethylene carbonate and diethyl carbonate (EC:DEC) with no additive yields a lower charge loss, while electrolytes containing 2 wt.% VC or FEC additives suffer from higher charge consumption for the formation and reformation of SEI due to higher solubility. To solely investigate stability and dissolution of the SEI in the absence of other ageing mechanisms, a model cell consisting of a carbon-coated aluminium foil working electrode and Prussian white counter and reference electrodes was used. Additionally, the experiments show a detrimental effect from using sodium metal counter electrodes. This work sheds light on the insufficiency of VC and FEC electrolyte additives in forming a perfect SEI. However, further investigations are required to account for additional ageing mechanisms to provide a comprehensive understanding of the role of VC and FEC in practical sodium-ion batteries.

Introduction

Sodium-ion batteries (SIBs) are strong alternatives to lithium-ion batteries (LIBs) and have been suggested as a drop-in replacement for LIBs in many applications. A key advantage over LIBs is that SIBs can be produced from more abundant materials. For example, Prussian blue analogue cathodes and bio-based hard carbon anodes could enable local production of battery active materials, strengthening supply resilience. LIBs are today the dominating battery technology due to superior energy density and stability. However, this is changing as more commercial SIBs are introduced to the market because of the high interest in lowering the cost while improving the sustainability of battery cells. In certain applications like stationary energy storage, it is possible to compromise on the energy density, but the stability and longevity of the SIBs are essential and should not be compromised.[1]

Carbonate-based electrolytes containing additives for the formation of an efficient solid electrolyte interphase (SEI) can achieve good cycling performance in full-cells.[2] Most reports focus on these carbonate-based electrolyte systems due to their favourable properties, particularly their high ionic conductivity and ability to form an efficient SEI, but also because they enable direct comparison with LIBs that use the same solvents. A “standard” electrolyte is based on a mixture of cyclic and linear carbonates. In many cases, ethylene carbonate (1,3-Dioxolan-2-one) and diethyl carbonate (EC:DEC) are mixed with 1 M $NaPF_6$ and film-forming additives like vinylene carbonate (VC) (1,3-Dioxol-2-one) and fluoroethyl carbonate (FEC) (4-Fluoro-1,3-dioxolan-2-one), which are employed to improve SEI efficiency and cycling performance. Nevertheless, forming a stable SEI in SIBs remains a critical issue, as there are conflicting results in the literature regarding how SEI stability can be improved.

In several hard carbon-based full-cell systems, the inclusion of FEC has increased the long-term cycling performance and improved SEI passivation compared to VC and additive-free baseline carbonate electrolytes, which suffer from gas evolution and higher irreversible capacity loss.[3–5] However, FEC is also known to cause voltage anomalies in Na-half cells, as well as causing performance loss with certain hard carbon electrodes compared to additive-free electrolytes.[6] Another issue is that the benefits provided by FEC are highly concentration-dependent and can either be beneficial or detrimental.[5]

Understanding all the SEI features is complex since it is difficult to investigate how the interplay between the electrodes and electrolyte affects SEI formation and the stability of the SEI layer under different conditions.[7] There is thus a great need for

electrochemical systems that can avoid complex and costly investigations of the electrode/electrolyte interphase in larger-scale battery testing, and preferably also allow separate investigations of different ageing mechanisms. The SEI is more than just a passive layer formed on the surface of the negative electrode. The formation and composition of the SEI is directly influenced by the electrolyte composition, cycling protocol, the electrode chemistry and morphology. As discussed in several reviews about battery ageing, it is quite difficult to gain a good understanding of all ageing mechanisms based only on cycling data of full-cells.[8–10]

For LIBs, model cells have been extensively employed. Martins et al. [11], for example, used model cells that employ a very representative surface layer of different graphite surfaces to model the chemical bonding environment that is found on top of the negative electrodes. These surfaces give very accurate insight into the SEI formation on the active material and allow investigation of certain mechanisms, like the interaction of water with the electrolyte. However, they struggle to provide a full picture of the SEI formation process because an applied composite electrode includes a current collector, multiple different carbon environments, as well as other functional groups that are not easily reproduced in the model cell. Additionally, these surfaces are difficult to prepare and must be handled with great care.[11]

For SIBs, previous studies using model cells have shown that a particular issue in SIBs is the dissolution of SEI species.[12,13] A few computational and experimental works have supported these finding showing that common SEI molecules like NaF and Na_2CO_3 are more soluble in carbonates than their lithium counterparts.[14–18] To study the stability and dissolution of SEI, we have developed different model systems.[19,20] The first effort aimed to investigate the effect of electrolyte additives on the SEI formation.[21] The results showed that the addition of even a small amount of a simple inorganic additive like NaF affects the SEI formation and its stability. For that work, a model cell using sodium metal as the counter electrode, a sodium conductive beta alumina as the separator, and platinum or gold as the working electrodes was employed.[21] The beta-alumina separator was used to eliminate the cross-talk between the electrodes, and metallic gold or platinum substrate allowed investigation of electrolyte reduction and stability of SEI in the absence of intercalation reactions. However, there are some downsides to this approach: (i) the low ionic conductivity of beta-alumina at room temperature limits the current that can be applied; otherwise, a significant overpotential would be observed; (ii) there is no additional reference electrode besides the sodium metal counter electrode which introduces spontaneous electrolyte reactions; (iii) the metallic substrate is chemically dissimilar from the actual substrates used in the battery cells which are mostly carbon-based.

Following this work, the model system was modified by replacing the beta alumina with a standard polymer-based separator and the use of a carbon black coated aluminium foil as the working electrode.[20] However, carbon black has some small reversible ion storage capacity, so diffusion-controlled ion trapping in addition to SEI formation and dissolution were investigated. However, the counter electrode was sodium metal, which is known to introduce electrolyte decomposition products into the electrolyte solution, thereby affecting the composition and properties of the SEI on the working electrode due to the cross-talk effects.[7,22,23]

Based on previous studies, we aimed to develop a model system that is easy to build from commercially available materials, enabling reproducible and reliable results without requiring significant time or financial investment. Here, we used a Prussian white (PW) electrode as the counter electrode, a partially desodiated PW as the reference electrode, and a carbon-coated aluminium foil as the working electrode. A carbonate-based electrolyte with and without electrolyte additives of VC or FEC was evaluated using three different cycling protocols of cyclic voltammetry (CV), galvanostatic cycling, and chronoamperometry.

Methods

All cells were built using custom pouch cells made of polymer-coated aluminium foil (Schematic seen in Figure 1a and S1). The polymer layer on the inside of the pouch insulated the current collectors cut from aluminium foil. All measurements were carried out in a three-electrode model cells schematically presented in Figure 1a and S1. Carbon-coated aluminium foil with 1 µm carbon coating and 15 µm substrate (MTI) was used as the working electrode. The counter electrodes used were PW double-sided coated (one side removed with deionised water, with the resultant single-sided electrode dried under vacuum at 140 °C for 14 hours) with an active mass loading of 9.8 mg/cm^2 coated on aluminium foil (12 µm) (Altris), or sodium metal chips (Xiamen AOT Electronics Technology). The reference electrodes were prepared by partially desodiating a PW electrode to the second plateau (66% of the theoretical capacity based on the active mass loading 9.8 mg cm^{-2}, assuming 150 mAh g^{-1}), providing reference electrodes with the potential of 3.3 V vs. Na^+/Na. The partially desodiated PW electrode was cut with a scissor in smaller pieces in a glovebox and introduced to the three-electrode cells. This means all replicas of a certain experiment were measured with similar reference electrodes. The counter electrode and the reference electrode were placed on the same side of the separator to simulate the increased resistance measured across the separator. Two layers of 19 mm diameter 2500 Celgard polypropylene were used as the separator (as seen in Figure 1a and Figure S1).

Electrolytes were prepared inside an argon-filled glovebox (O_2 and H_2O < 1 ppm) by first mixing EC and DEC in a 1:1 volume ratio and drying them over molecular sieves for at least 48 hours. Solvents, salts, and additives were acquired, if possible, in the battery grade quality: ethylene carbonate (Gotion), diethyl carbonate (Gotion), fluoroethylene carbonate (Sigma Aldrich), vinylene carbonate (Sigma Aldrich), and sodium hexafluorophosphate (Solvionic, used as received).

View Article Online
DOI: 10.1039/D6FD00058J

Dried solvents were mixed with $NaPF_6$ salt inside a glass volumetric bottle, yielding 1 molar solutions. The salt was dissolved before adding enough solvent to reach the demarcation line for the final total volume. The base electrolyte was then transferred for storage to stainless steel bottles with silicone rubber seals and plastic caps. 2 wt.% FEC or 2 wt.% VC were added into the base electrolyte to prepare additional electrolyte solutions.

Three different cycling protocols were tested: (i) CV for two cycles (scan rate 0.1 mV s^{-1} from OCV to 0.3 V to 2.2 V vs. Na^+/Na) to test initial SEI formation followed by a 50-hour pause to evaluate whether the SEI dissolves, followed by two subsequent CV cycles (Figure 1b); (ii) galvanostatic cycling with 3 µA (2.25 µA cm^{-2}) applied for six cycles followed by 50-hour pause and six more cycles to see if SEI formed under current controlled conditions is similar to the CV case (Figure 1c); and (iii) chronoamperometry at a potential hold of 300 mV vs. Na^+/Na for 40 hours to investigate if low voltage storage would yield to different dissolution and reformation rates with subsequent CV scanning to evaluate the passivation (Figure 1d). After demonstrating the ability of this system to mirror the SEI formation, we investigated the impact of VC and FEC on the passivation and ageing of the SEI in this model system.

GC-MS and XPS measurements were carried out on 4 additional cells using 1 M $NaPF_6$ EC:DEC with and without 2 wt.% VC electrolytes with PW or Na-metal counter electrodes. The methodology and results are discussed in detail in the supporting information. In brief, after one CV cycling as shown in Figure S2a, the cells were cut open inside an argon-filled glovebox, and the working electrodes and separators were immersed in 1 mL dimethyl carbonate (DMC) to dissolve remaining salt. The obtained DMC solution was then diluted with dichloromethane, centrifuged, and analysed by GC-MS to separate and identify the electrolyte components and possible degradation products.

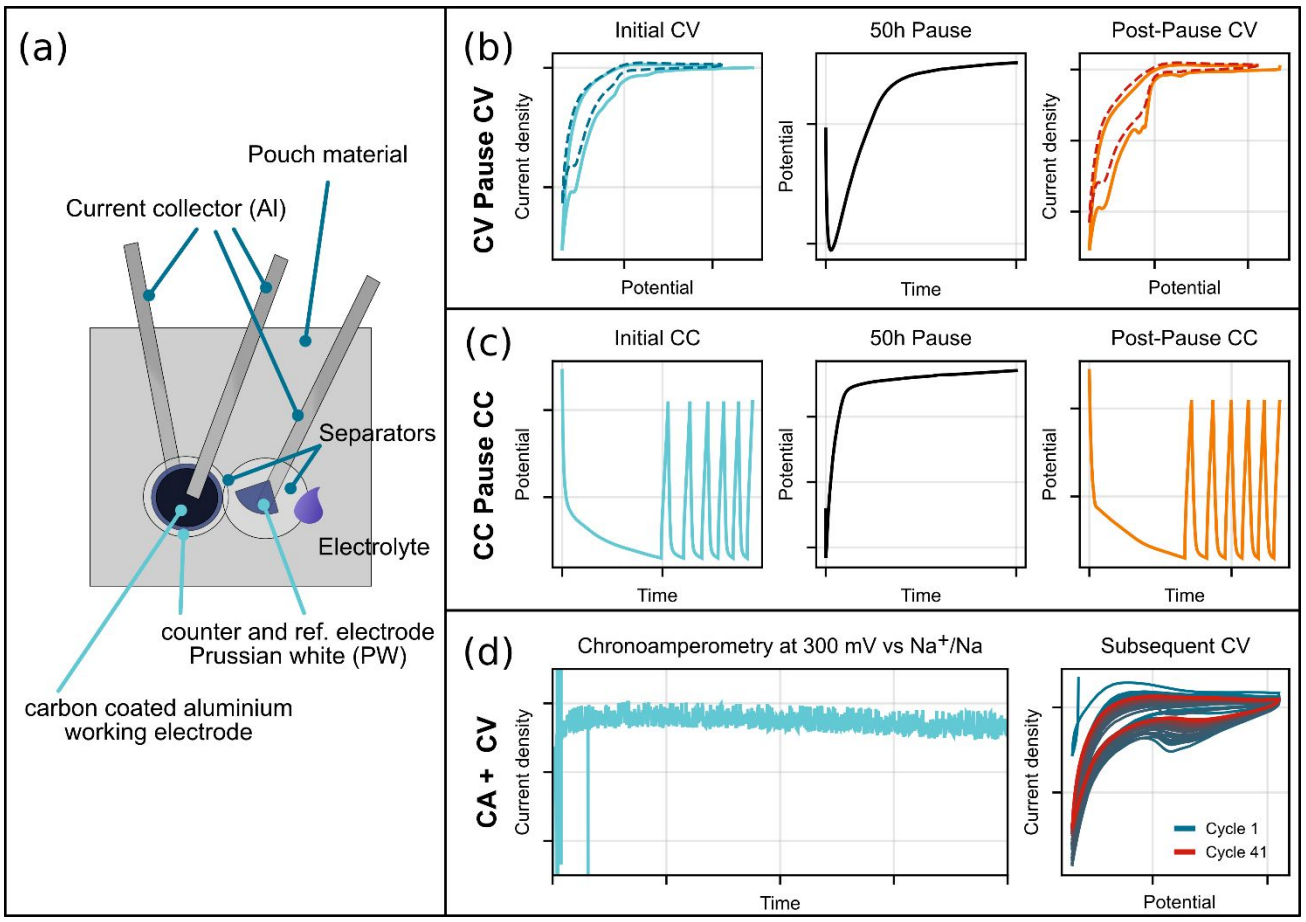

Figure 1: a) Schematic of the model cells using a carbon-coated aluminium foil as the working electrode, a pristine Prussian white electrode as the counter electrode, and a partially desodiated Prussian white electrode (at 3.3 V vs. Na^+/Na) as the reference electrode. The working electrode is carbon-coated on a metal substrate on which the SEI is formed. Cells were tested with three different protocols, and here the schematic cycling protocols are shown without detailed axis and data labelling, b) CV for two scans followed by a 50-hour pause and two more scans, c) Galvanostatic cycling for six cycles followed also by a 50-hour pause and six more cycles. d) Chronoamperometry (at 300 mV vs. Na^+/Na for 40 hours) followed by subsequent CV.

Results

Here, we present results regarding the formation and stability of the SEI in 1 M $NaPF_6$ EC:DEC (1:1 v:v) electrolyte with and without VC or FEC additive using a model cell (Figure 1a). Three different electrochemical cycling methods were used (see Figure 1b-d), and each experiment was repeated to discuss the reliability of the model cell data. The CVs of the cells using the electrolyte with no additives show small features between 0.9 and 0.3 V (all the potential values are hereafter presented vs. Na^+/Na), see Figure 2a. However, there are significant reduction peaks observed at around 1 V for both VC and FEC containing electrolytes. The reduction of VC and FEC are the dominant electrochemical reactions; thus, the small reduction features observed for the additive-free electrolyte are not detectable in the additive-containing electrolytes. The integrated reduction capacities show that passivation is present as the capacities are decreased from the first to the second cycle, see Figure 2b. However, the reduction capacity is again increased after the 50-hour pause. This reveals that part of the SEI formed during the reduction is consequently dissolved into the electrolyte solutions or detached from the substrate during the pause. The oxidation capacity is almost zero, indicating that no significant oxidation of SEI occurs. The observed potentials for FEC reduction are similar to reported values in the literature, stating that the onset for degradation is around 1 V.[24] The reduction potential of VC is similarly very close to the expected value.

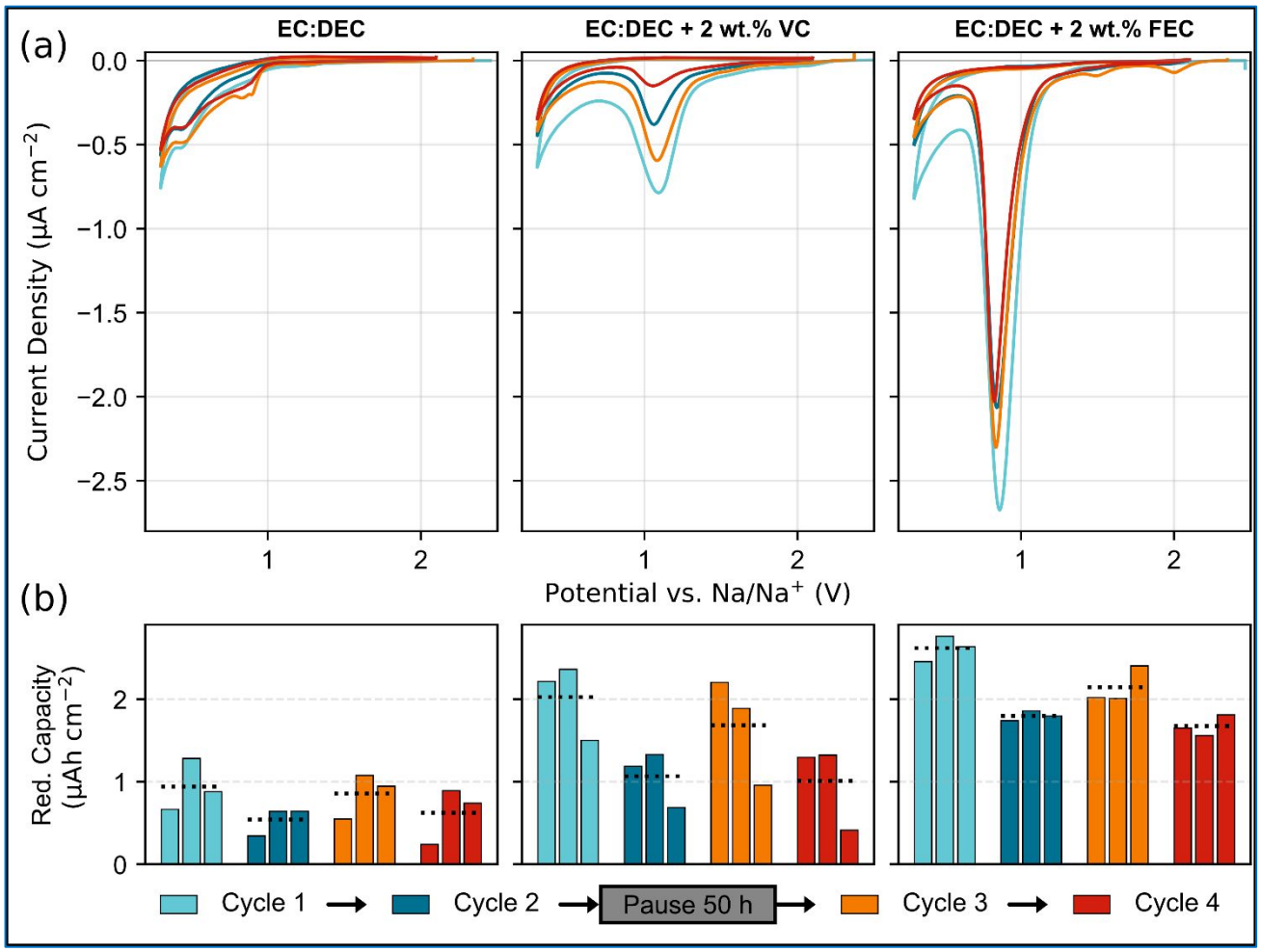

Figure 2: a) CVs of model cells using carbon-coated aluminium working electrode and a Prussian white counter electrode in 1 M $NaPF_6$ EC:DEC (1:1 v:v) with and without 2 wt.% of either VC or FEC cycled between 0.3 V and 2.2 V vs. Na^+/Na. The initial cycles (in light blue and dark blue) were followed by a 50-hour pause and two subsequent cycles (third cycle in orange and fourth in red). b) Integrated reduction capacity in µAh cm^{-2} shown as bars in the same colours as in a). Each bar of the same colour represents one replica (three replicas per electrolyte) with the average shown as a dotted line.

A similar experiment was performed using sodium metal instead of PW as the counter electrode, see Figure 3. The CVs show no distinct reduction peak for VC, indicating that the sodium metal counter electrode consumed all or part of VC during the 10-hour resting period before cycling. To gain further understanding of the degradation behaviour of VC and the influence of the sodium metal counter electrode, further experiments were made (see supporting information methods, results sections, as well as Figure S2a). In short, 4 cells with the same configurations as shown in Figure 3 (a) were run for one formation cycle. The

View Article Online
DOI: 10.1039/D6FD00038J

electrodes were immersed in DMC, after which the washing liquid was analysed using GC-MS, and the electrode surfaces were analysed by XPS. Based on the GC-MS analysis, VC remained present in both the VC-containing cells (with PW or Na-metal counter electrodes, see Figure S2c), indicating that it was only partially, rather than fully, consumed by the sodium metal. The decrease in the concentration of VC and thus changes in the solvation structure likely explain why no VC reduction peak was observed in CV results. An additional measurement was done increasing the VC concentration to 10% wt.% (Figure S3). These results showed a clear VC decomposition peak, revealing that consumption of VC by sodium metal is limited, hence higher concertation of VC results in a clear reduction peak of VC on the working electrode.

It is evident that the counter electrode has a significant impact on the SEI formation. The presence of a reactive counter electrode such sodium metal can alter the electrolyte composition, as shown here by the partial consumption of VC. In addition, species generated from electrolyte decomposition due to reaction with sodium metal may migrate to the surface of the working electrode, thereby modifying the SEI composition, as evidenced by the XPS results in Figure S2b.

Also, the sodium metal-containing cells show higher variation in the reduction capacity compared to the cells with PW counter electrode, see Figure 2b. This suggests that the reaction between the electrolyte and sodium metal results, and the resulting species formed, are not necessarily reproducible.

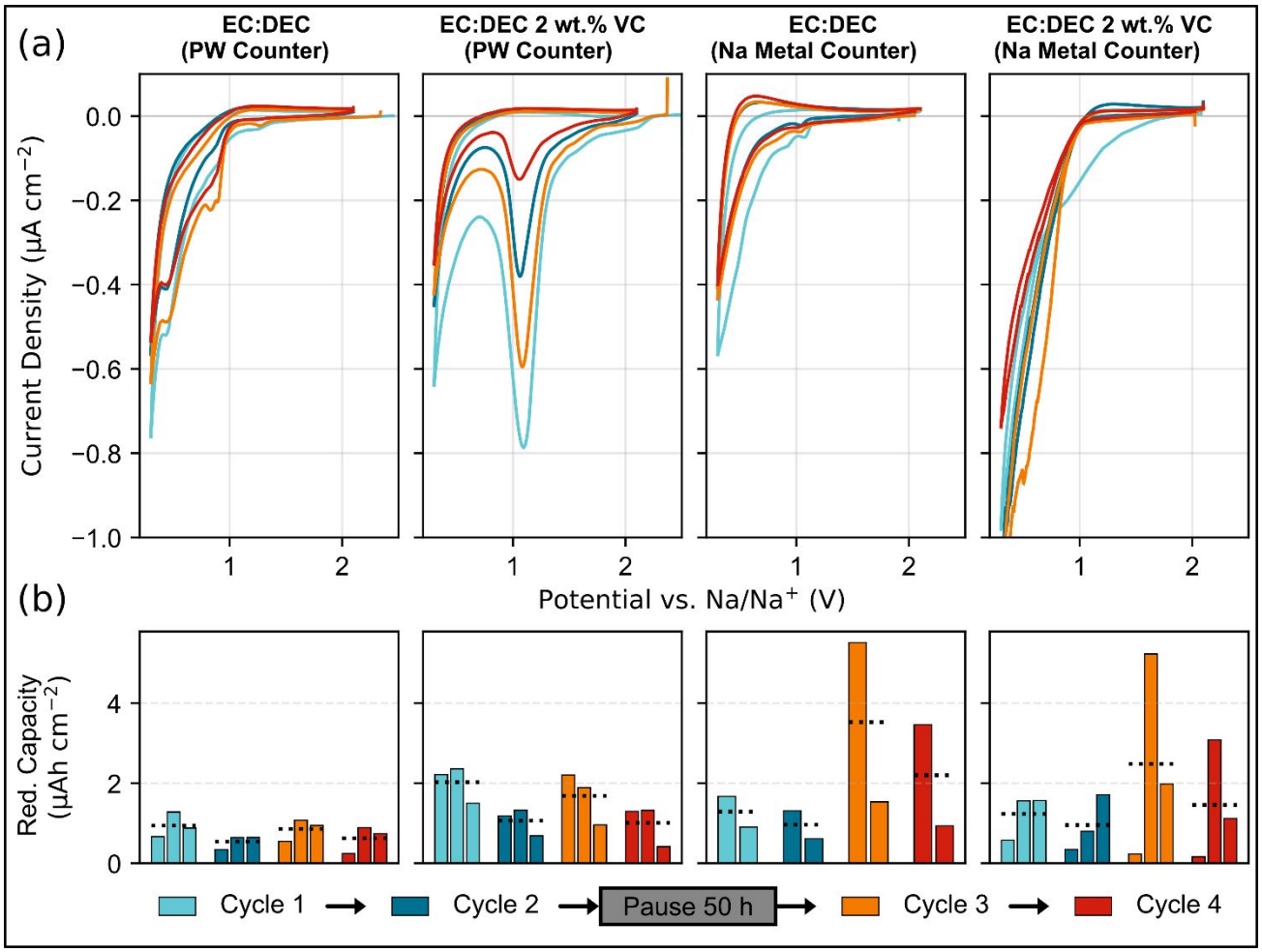

Figure 3: a) CVs of model cells using a carbon-coated aluminium working electrode and a Prussian white counter electrode in 1 M $NaPF_6$ EC:DEC (1:1 v:v) with and without 2 wt.% VC with Prussian white and sodium metal counter electrodes cycled between 0.3 V and 2.2 V. The initial cycles (in light blue and dark blue) are followed by a 50-hour pause and two subsequent cycles (3rd cycle in orange and 4th in red). b) The reduction capacity in µAh cm^{-2} shown as bars in the same colours as in a). The bars with the same colour represent replicas (three replicas per electrolyte) with the average capacity shown as a dotted line. The data shown for the PW counter are also shown in Figure 1 and displayed for comparison.

The constant current experiments (Figure 4) show a slightly different outcome compared to the CVs. Here, the electrolyte with no additives showed the lowest capacity, which is in line with the results from the CV. After the 50-hour pause, the VC-containing cells showed a slight increase in reduction capacity (Figure 4 b VC containing cells average reduction capacity is higher after 50 h pause (orange and red bars)), which indicates that the SEI formed in the VC-containing electrolyte largely diminished during the pause time. The FEC-containing cells had the highest initial reduction capacity and showed increased reduction capacity after a 50-

hour pause. However, opposite to the VC containing electrolyte, the capacity decreased with each cycle. In the VC case, the reduction capacities before and after the pause remained the same.

View Article Online
DOI: 10.1039/D6FD00038J

There is very little oxidative current in the voltage range of the constant current experiments; this can also be seen in the CV scans (Figure 2). This is a strong indication that the SEI formed is stable under oxidative conditions and that there is no reversible sodium intercalation or other reversible reactions.

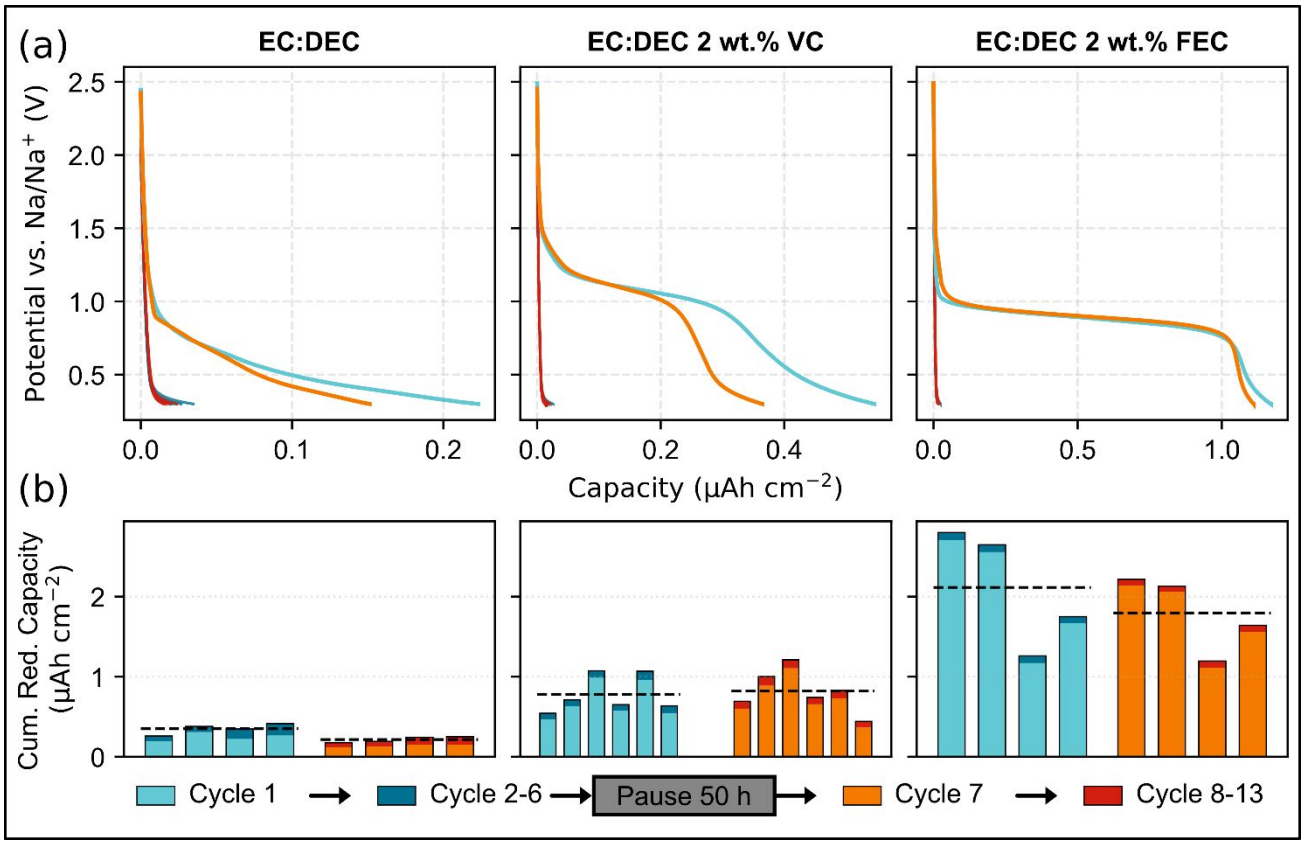

Figure 4: a) Potential vs. areal capacity (µAh cm^{-2}) of model cells using 1 M $NaPF_6$ EC:DEC (1:1 v:v) electrolyte with and without 2 wt.% of either VC or FEC cycled between 0.3 V and 2.4 V. All models cells have a carbon coated aluminium working- and a Prussian white counter-electrode. The first cycle (in light blue) is followed by cycles 2 to 6 (dark blue), a 50-hour pause and subsequent cycles (7th in orange and 8th-13th in red). b) Reductive areal capacity in µAh cm^{-2} shown as bars in the same colours as in a). Each bar of the same colour represents one replica (four or six replicas per electrolyte) with the average shown as a dotted line. Reduction capacities for cycles 2-6 and 8-13 are shown on top of the initial formation and reformation capacity.

To investigate whether SEI dissolution would stop at some point and thus if the carbon-coated aluminium would reach a fully passivated state, continuous CV scans were performed for 45 cycles (see Figure 5). The results show that the additive-free electrolyte reached a "stable" state after the first few cycles, whereas it took more cycles for the VC-containing electrolyte to reach significantly lower reduction capacity. The issue was more severe for the FEC-containing electrolytes, as it exhibited relatively large reduction capacities for more than 30 cycles (Figure 5b).

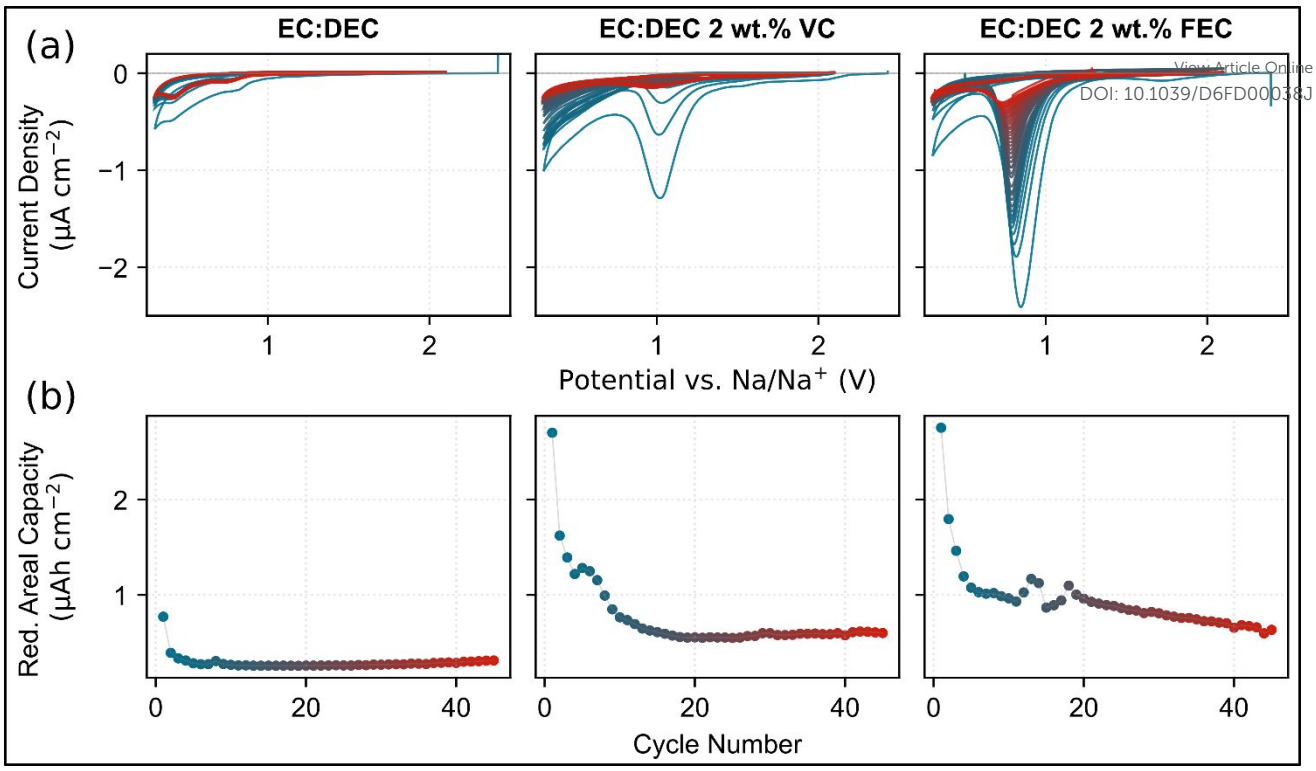

Figure 5: a) Continuous CV scanning of the carbon-coated aluminium working electrode (Prussian white counter electrode) in 1 M $NaPF_6$ EC:DEC (1:1 v:v) electrolyte with and without 2 wt.% of either VC or FEC. Initial CV scans are shown in dark blue and gradually shift to red as the cycle number increases. b) Areal reduction capacity (from the CV cycling) as a function of the cycle number.

In a chronoamperometry experiment, the working electrode was kept at a constant potential of 300 mV for around 50 hours to see if there was a change in the current. The cells with the additive-free electrolyte showed no significant differences except for one outlier cell (Figure 6 and replicas shown in Figure S5). The noise level was about 1 μA $cm^{-2,}$ which is the same magnitude as one would expect based on the previous CV and galvanostatic cycling experiments. There was also a large signal in the middle of the potential step hold, which is attributed to a potentiostat error. To test the SEI stability after the 40-hour constant potential step, the cells underwent subsequent CV cycling. It is apparent that the additive-free electrolyte did not undergo further passivation, and the CV behaviour remained consistent over 40 subsequent cycles. The VC- and FEC-containing cells showed similar potential step responses, but the CV revealed that additional reactions took place after the potential step (Figure 6b and c). The initial CV cycles following the potential step (blue) showed a similar behaviour to the voltammograms seen in the continuous CV experiments after 10 cycles for the VC and more than 40 cycles for the FEC. This indicates that the potential step indeed formed a passivating SEI, but in the FEC- and VC-containing cells, the current increased and the typical decomposition peak reappeared in the FEC system, as well as to a minor extent in the VC system.

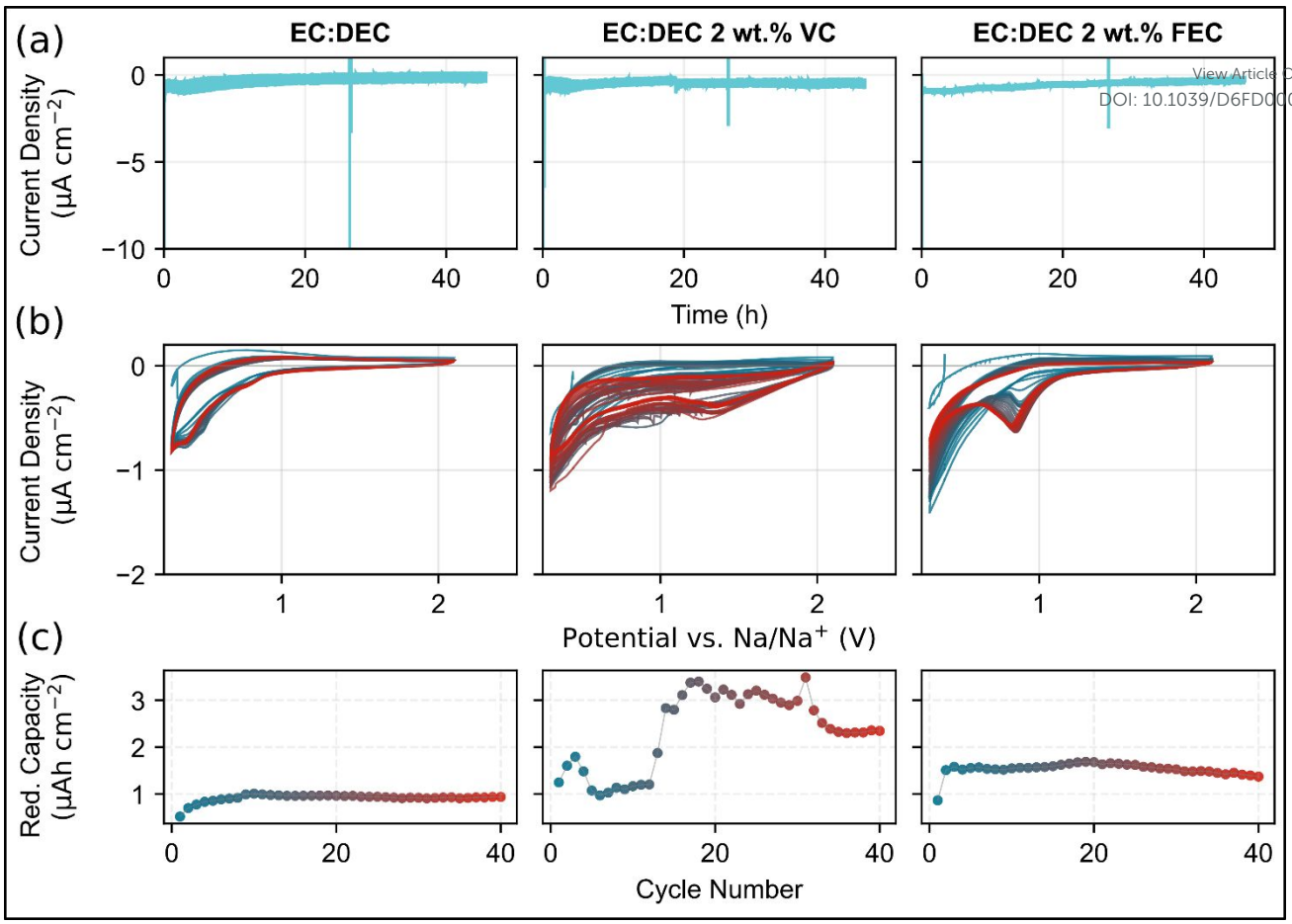

Figure 6: a) Areal current density of a potential step of 300 mV for more than 40 hours recorded on a carbon-coated working electrode in 1 M $NaPF_6$ EC:DEC (1:1 v:v) with and without 2 wt.% of either VC or FEC. b) Subsequent testing of the SEI stability by continuous CV cycling. c) Areal reduction capacity versus cycle number (cycle numbers shown as a gradient from dark blue (cycle 1) to red (cycle 40))

Discussion

Based on the results presented above, we report that there is constant dissolution and SEI reformation in all of the electrolytes tested. Furthermore, there is no improvement using VC and FEC. This means that the mainly organic SEI derived from VC or the hybrid inorganic/organic SEI associated with FEC is not enough to stop the further degradation of EC and DEC. The VC decomposition peak disappears after five cycles, but there is still a higher reformation capacity in every following cycle (Figures 5 and 6). After that, the CV current profile is similar to that for EC:DEC, which indicates that the VC SEI is not enough to stop EC:DEC decomposition. In the case of FEC, we can verify previous work showing that the SEI, formed with low concentrations (2 wt.%), is not passivating, and the FEC is continuously being reduced over 40 CV scans.

The continuous SEI formation and dissolution (Figures 2, 3 and 4) in the baseline electrolyte can be explained by the constant reduction of DEC and EC, yielding mainly organic species. These organic SEI components have high solubilities, as should be expected since the degradation products of EC and DEC should include dimers and organic molecules very similar to the solvents.[26,27] These degradation products were observed by XPS and GC-MS in EC:DEC electrolyte with Na-metal counter electrode and indicated that chemical reactions happen, forming SEI and also dissolution products (see Figure S2 b and c). Continuous solvent reactions were also shown by Hu et al.[28], indicating that the formation of oligomers through solution-phase chemical chain reactions poses a massive challenge in sodium and potassium systems. These chain reactions are initiated by nucleophilic ethoxides, which are generated during the degradation of DEC. The ethoxide intermediates in sodium systems exhibit higher nucleophilicity compared to lithium analogues and continuously attack intact solvent molecules (EC and DEC), producing large amounts of soluble oligomers and alkali metal alkyl carbonates.[28] Our model system indicates that these ethoxide-induced side reactions are not inhibited by the presence of traditional film-forming additives like VC or FEC. These solvent-consuming organic chain reactions appear to be the primary driver for the continuous SEI dissolution and reformation observed at the anode. One can note that VC also passivates the Na-metal surface, based on XPS and GC-MS results. The surface of the working electrode and the GC-MS analysis show now additional degradation products (Figure S2). If added in sufficient amounts (10 wt.%) VC shows a

View Article Online
DOI: 10.1039/D6FD00038J

reduction peak in the presence of sodium metal (Figure S3). This shows that the metal counter will change the electrochemical results, but it also shows that the concentration of the additive is critical. Further experiments should be conducted if similar behaviour can be seen with other additives.

The inorganic SEI should contribute very little to the dissolution process. Most reports[4,16] name NaF and Na_2CO_3 as the major inorganic constituents of the SEI, and those have very low solubilities in EC:DEC (3.057 and 3.648 mg L^{-1})[21]. If NaF and Na_2CO_3 take part in one and two-electron degradation reactions, one would expect a capacity of 0.195 and 0.184 µAh to saturate a 100 µL solution of EC:DEC. This is a fraction of the capacity observed in the first cycle of the SEI formation in all the cells and protocols tested. So even if the inorganic SEI is formed during the first cycle, it does not decrease the constant degradation of solvents and the dissolution of the organic SEI parts. If the inorganic SEI is contributing to the constant reformation capacity, another mechanism might be at play. This work only tested two substrates (CC-Al and CC-Cu, Figure S4), and even between these two substrates, there are large differences. This does not imply that the results are not valid for the main work (CC-Al), but it makes clear how specific the SEI formation is and that a different current collector metal can influence the reduction current and reversible current observed in such a model system. For example, copper oxide will undergo redox reactions in the presence of sodium (see SI for more detailed discussion and Figure S5). This fact makes it difficult to compare lithium and sodium SEI formation because it is hard to find a system that does not have additional reactions besides the SEI formation and still allows comparison between the two alkali metals.

An important note to make for future investigation is that sodium metal will influence the SEI formation by spontaneous SEI formation, as shown in Figure 3, where VC is consumed before it can be reduced on the anode. One should avoid testing electrolytes and additives in systems containing sodium metal counter electrodes if the electrolyte is to be employed in a system where no or little sodium metal will be present. Sodium metal will influence the behaviour of the SEI formation and stability. As seen in Figure 3, the presence of a sodium metal counter electrode changed the behaviour of the VC-containing electrolyte. The clear decomposition peak of VC observed when using PW disappears. The assumption is that VC spontaneously reacts with the sodium metal surface. It is a clear indication that testing electrolytes for full cell operation should be done with full cell materials or inert materials with low or no chemical side reactions.[29]

The reported results are consistent over three different electrochemical techniques with multiple replicas. As seen in Figure 3, the initial formation measurements with a 50-hour pause were recorded for the three electrolytes with three or more replicas. These indicate the same trends for the galvanostatic cycling and CV experiments. All the extra experiments were done with at least one repeat (most of them with three replicas). There are some clear outliers in these measurements, which can be explained by the very low surface area – this means that the system is highly sensitive to any surface defects or impurities introduced during the handling and assembly of the pouch cells. It has to be noted that the FEC-containing system shows the most reproducible behaviour among all the experiments.

Conclusions

Clear SEI formation is observed in a series of electrochemical experiments employing a model system containing a carbon-coated aluminium foil working electrode and a stable counter and reference electrode of Prussian white. In contrast to full cell data, we report that the best negative electrode SEI stability on carbonaceous electrodes is achieved with a simple 1 M NaPF6 EC:DEC mixture, and that adding either 2 wt.% of VC or FEC has a negative impact on the stability. We report higher initial formation capacities and higher SEI reformation capacities in a voltage range from 2.4 to 0.3 V. This higher reformation reduction capacity means that a lower columbic efficiency would be recorded in full cells. While a clear decomposition of these additives is observed, the expected passivation is only achieved on short-term cycling but not during long-term testing. The chosen model system with Prussian white counter and reference electrodes shows high reproducibility for CV, galvanostatic and chronoamperometry experiments and the trend is observed across these different protocols for multiple replicas.

Based on the CV experiments, the SEI is continuously dissolving, so that the passivation is never completed, and a few cycles are not enough to passivate the carbon-coated substrates. Even after long-term cycling (40 CV scans at 0.1 mV/s), a reductive capacity is still observed, which is higher for VC and FEC-containing cells than for 1 M $NaPF_6$ EC:DEC.

Sodium metal electrodes clearly affect the SEI formation in the tested electrolytes, altering the passivation behaviour by reacting chemically with the electrolyte and therefore influencing the stability either through crosstalk or through consumption of the film-forming additives. Whenever electrolytes designed for intercalation materials are tested, one should refrain from using sodium metal.

Data availability

The data supporting this article have been included as part of the supporting Information. Supporting information, including additional cyclic voltammetry results of different substrates, electrolytes, CVs of cells containing Sodium metal counter electrodes, potential step results and GC-MS/XPS results.

Data for this article, metadata of the battery cells cycled, all electrochemical, XPS and GC-MS data collected in the frame of this project are available at Zenodo at [URL – format https://doi.org/DOI].

View Article Online
DOI: 10.1039/D6FD00038J

Author contributions

J. F. Schuster, conceptualisation, data curation, formal analysis, investigation, methodology, visualisation, writing original draft
Q. Hu, validation, investigation (model cells with Prussian white counter)
L. J. King, data curation (XPS), formal analysis (XPS), methodology (XPS)
A. Lapidus, validation, investigation (model cells with sodium metal counter)
C. A. Hall, conceptualisation, writing – review & editing
L. Nyholm, conceptualisation, writing – review & editing
R. Younesi, conceptualisation, writing – review & editing, supervision, resources, funding acquisition

Conflicts of interest

Reza Younesi is a co-founder of the Company Altris, which provided the Prussian White electrodes for this research work. All other authors declare no conflict of interest.

Acknowledgements

The authors thank Júlia Costa Rodriguez for assembling full cells and cycling them. Meghdad Hosseinzadegan is acknowledged for valuable discussions on SEI formation and dissolution involving sodium metal. Financial support from STandUP for energy is also acknowledged.

References

1 N. Tapia-Ruiz, A. R. Armstrong, H. Alptekin, M. A. Amores, H. Au, J. Barker, R. Boston, W. R. Brant, J. M. Brittain, Y. Chen, M. Chhowalla, Y.-S. Choi, S. I. R. Costa, M. C. Ribadeneyra, S. A. Cussen, E. J. Cussen, W. I. F. David, A. V. Desai, S. A. M. Dickson, E. I. Eweka, J. D. Forero-Saboya, C. P. Grey, J. M. Griffin, P. Gross, X. Hua, J. T. S. Irvine, P. Johansson, M. O. Jones, M. Karlsmo, E. Kendrick, E. Kim, O. V. Kolosov, Z. Li, S. F. L. Mertens, R. Mogensen, L. Monconduit, R. E. Morris, A. J. Naylor, S. Nikman, C. A. O'Keefe, D. M. C. Ould, R. G. Palgrave, P. Poizot, A. Ponrouch, S. Renault, E. M. Reynolds, A. Rudola, R. Sayers, D. O. Scanlon, S. Sen, V. R. Seymour, B. Silván, M. T. Sougrati, L. Stievano, G. S. Stone, C. I. Thomas, M.-M. Titirici, J. Tong, T. J. Wood, D. S. Wright and R. Younesi, *J. Phys. Energy*, 2021, **3**, 031503.
2 D. Monti, E. Jónsson, A. Boschin, M. R. Palacín, A. Ponrouch and P. Johansson, *Phys. Chem. Chem. Phys.*, 2020, **22**, 22768–22777.
3 A. Fordham, D. Wee, R. E. Owen, T. Luo, R. Jackowska, T. Jia, Y. Zheng, E. Kendrick, W. M. Dose, D. J. L. Brett, P. R. Shearing, J. B. Robinson and R. Jervis, *EES Batteries*, 1447, **2**, 253–269.
4 J. Fondard, E. Irisarri, C. Courrèges, M. R. Palacin, A. Ponrouch and R. Dedryvère, *J. Electrochem. Soc.*, 2020, **167**, 070526.
5 A. Bouibes, N. Takenaka, K. Kubota, S. Komaba and M. Nagaoka, *RSC Advances*, 2022, **12**, 971–984.
6 R. Dugas, A. Ponrouch, G. Gachot, R. David, M. R. Palacin and J. M. Tarascon, *J. Electrochem. Soc.*, 2016, **163**, A2333.
7 C. Bommier and X. Ji, *Small*, 2018, **14**, 1703576.
8 J. S. Edge, S. O'Kane, R. Prosser, N. D. Kirkaldy, A. N. Patel, A. Hales, A. Ghosh, W. Ai, J. Chen, J. Yang, S. Li, M.-C. Pang, L. Bravo Diaz, A. Tomaszewska, M. W. Marzook, K. N. Radhakrishnan, H. Wang, Y. Patel, B. Wu and G. J. Offer, *Phys. Chem. Chem. Phys.*, 2021, **23**, 8200–8221.
9 X. Han, L. Lu, Y. Zheng, X. Feng, Z. Li, J. Li and M. Ouyang, *eTransportation*, 2019, **1**, 100005.
10 M. Hashimov and A. Hofmann, *Batteries*, 2023, **9**, 530.
11 M. Martins, D. Haering, J. G. Connell, H. Wan, K. L. Svane, B. Genorio, P. Farinazzo Bergamo Dias Martins, P. P. Lopes, B. Gould, F. Maglia, R. Jung, V. Stamenkovic, I. E. Castelli, N. M. Markovic, J. Rossmeisl and D. Strmcnik, *ACS Catal.*, 2023, **13**, 9289–9301.
12 R. Mogensen, D. Brandell and R. Younesi, *ACS Energy Lett.*, 2016, **1**, 1173–1178.
13 M. Moshkovich, Y. Gofer and D. Aurbach, *J. Electrochem. Soc.*, 2001, **148**, E155.
14 G. G. Eshetu, S. Grugeon, H. Kim, S. Jeong, L. Wu, G. Gachot, S. Laruelle, M. Armand and S. Passerini, *ChemSusChem*, 2016, **9**, 462–471.
15 N. Xin, Y. Sun, M. He, C. J. Radke and J. M. Prausnitz, *Fluid Phase Equilibria*, 2018, **461**, 1–7.
16 G. G. Eshetu, G. A. Elia, M. Armand, M. Forsyth, S. Komaba, T. Rojo and S. Passerini, *Advanced Energy Materials*, 2020, **10**, 2000093.
17 K. Hankins, M. H. Putra, J. Wagner-Henke, A. Groß and U. Krewer, *Advanced Energy Materials*, 2401153.
18 J. Timhagen, V. Thangavel, J. Forero-Saboya, J. Weidow and P. Johansson, *Electrochimica Acta*, 2025, **539**, 147051.
19 J. F. Schuster, L. A. Ma, C. A. O'Keefe, C. P. Grey and R. Younesi, *Energy Adv.*, 2026, **5**, 146–150.
20 L. A. Ma, A. Buckel, A. Hofmann, L. Nyholm and R. Younesi, *Advanced Science*, 2024, **11**, 2306771 (1–10).
21 L. A. Ma, A. J. Naylor, L. Nyholm and R. Younesi, *Angewandte Chemie*, 2021, **133**, 4905–4913.
22 J. R. Fitzpatrick, B. E. Murdock, P. K. Thakur, T.-L. Lee, S. Fearn, A. J. Naylor, D. Biswas and N. Tapia-Ruiz, *Advanced Science*, 2025, **12**, e04717.
23 E. Björklund, D. Brandell, M. Hahlin, K. Edström and R. Younesi, *J. Electrochem. Soc.*, 2017, **164**, A3054.

24 S. Komaba, T. Ishikawa, N. Yabuuchi, W. Murata, A. Ito and Y. Ohsawa, *ACS Appl. Mater. Interfaces*, 2011, **3**, 4165–4168.
25 L. E. Ouatani, R. Dedryvère, C. Siret, P. Biensan, S. Reynaud, P. Iratçabal and D. Gonbeau, *J. Electrochem. Soc.*, 2008, **156**, A103.
26 A. Hofmann, F. Müller, S. Schöner and F. Jeschull, *Batteries & Supercaps*, 2023, **6**, e202300325.
27 A. Bouibes, N. Takenaka, T. Fujie, K. Kubota, S. Komaba and M. Nagaoka, *ACS Appl. Mater. Interfaces*, 2018, **10**, 28525–28532.
28 J. Hu, H. Wang, F. Yuan, J. Wang, H. Zhang, R. Zhao, Y. Wu, F. Kang and D. Zhai, *Nano Lett.*, 2024, **24**, 1673–1678.
29 K. Cui, R. Hou, H. Zhou and S. Guo, *Advanced Functional Materials*, 2025, **35**, 2419275.